

BCL11B Regulates Arterial Stiffness and Related Target Organ Damage

Jeff Arni C. Valisno¹, Joel May¹, Kuldeep Singh², Eric Y. Helm³, Lisia Venegas¹, Enkhjargal Budbazar¹, Jena B. Goodman¹, Christopher J. Nicholson², Dorina Avram^{3,4}, Richard A. Cohen¹, Gary F. Mitchell⁵, Kathleen G. Morgan², Francesca Seta^{1*}

¹ Vascular Biology Section, Department of Medicine, Boston University School of Medicine, Boston, MA, USA; ² Department of Health Sciences, Sargent College, Boston University, Boston, MA, USA; ³ Department of Anatomy and Cell Biology, College of Medicine, University of Florida, Gainesville, FL, USA; ⁴ Department of Immunology, Moffitt Cancer Center, Tampa, FL, USA
⁵ Cardiovascular Engineering, Norwood, MA, USA.

* corresponding author

Running title: Smooth Muscle BCL11B Regulates Vascular Function



Circulation Research

Subject Terms:

Animal Models of Human Disease
Basic Science Research
Vascular Biology
Vascular Disease

Address correspondence to:

Dr. Francesca Seta
Boston University School of Medicine
Department of Medicine,
Vascular Biology Section
650 Albany Street, X720
Boston MA 02118
Tel: (+1) 613-358-7814
setaf@bu.edu

This article is published in its accepted form. It has not been copyedited and has not appeared in an issue of the journal. Preparation for inclusion in an issue of *Circulation Research* involves copyediting, typesetting, proofreading, and author review, which may lead to differences between this accepted version of the manuscript and the final, published version.

ABSTRACT

Rationale. B-cell leukemia 11b (BCL11B) is a transcription factor known as an essential regulator of T lymphocytes and neuronal development during embryogenesis. A genome-wide association study (GWAS) showed that a gene desert region downstream of *BCL11B*, known to function as a *BCL11B* enhancer, harbors single nucleotide polymorphisms (SNPs) associated with increased arterial stiffness. However, a role for BCL11B in the adult cardiovascular system is unknown.

Objective. Based on these human findings, we sought to examine the relation between BCL11B and arterial function.

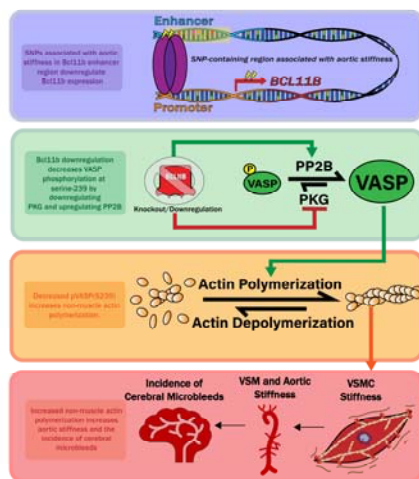
Methods and Results. Here we report that BCL11B is expressed in the vascular smooth muscle (VSM) where it regulates vascular stiffness. RNA sequencing of aortas from WT and *Bcl11b* null mice (BSMKO) identified the cyclic guanosine monophosphate (cGMP)-protein kinase G (PKG) as the most significant differentially regulated signaling pathway in BSMKO compared to WT mice. BSMKO aortas showed decreased levels of PKG1, increased levels of Ca⁺⁺-calmodulin-dependent serine/threonine phosphatase calcineurin (PP2B) and decreased levels of their common phosphorylation target, vasodilator-stimulated phosphoprotein (pVASP^{S239}), a regulator of cytoskeletal actin rearrangements. Decreased pVASP^{S239} in BSMKO aortas was associated with increased actin polymerization (F/G actin ratio). Functionally, aortic force, stress, wall tension and stiffness, measured *ex vivo* in organ baths, were increased in BSMKO aortas, and BSMKO mice had increased pulse wave velocity, the *in vivo* index of arterial stiffness. Despite having no effect on blood pressure or microalbuminuria, increased arterial stiffness in BSMKO mice was associated with increased incidence of cerebral microbleeds compared to age-matched WT littermates.

Conclusions. We have identified VSM BCL11B as a crucial regulator of aortic smooth muscle function and a potential therapeutic target for vascular stiffness.

bioRxiv: <https://www.biorxiv.org/content/10.1101/193110v1>

Keywords:

Vascular smooth muscle cells, arterial stiffness, vascular function, cerebral microbleeds, BCL11B, aortic stiffness.



Nonstandard Abbreviations and Acronyms:

BCL11B	B-cell leukemia 11b
BSMKO	tamoxifen-inducible VSM-specific <i>Bcl11b</i> null mice
CTIP2	COUP-TF interacting protein-2
GWAS	genome-wide association study
HFHS	high-fat, high-sucrose
KHB	Krebs-Henseleit buffer
ND	normal diet
SNPs	single nucleotide polymorphisms
PKA	cAMP-dependent protein kinase A
PKG1	cGMP-dependent protein kinase isoform 1
PP2B	Ca ²⁺ /calmodulin dependent serine-threonine phosphatase calcineurin
PWV	pulse wave velocity
VASP	vasodilator-stimulated phosphoprotein
VSM	vascular smooth muscle

INTRODUCTION

Cardiovascular disease (CVD) morbidity and mortality remain a dire public health burden, claiming more lives each year than all forms of cancer combined¹. Loss of compliance of large elastic arteries, also known as arterial stiffening, is a strong independent risk factor for CVD. Carotid-femoral pulse wave velocity (PWV), the gold standard clinical measure of aortic wall stiffness², predicts incident hypertension³⁻⁵, heart failure, stroke and coronary artery disease^{2,6-9} and cognitive decline¹⁰, independently of other CVD risk factors. Moreover, recent evidence suggests that increased pressure pulsatility due to large artery stiffness can lead to end-organ microcirculatory injury, potentially inciting structural and functional changes in organ systems, referred to as target-organ damage (TOD). TOD is highly associated with, and considered a precursor of, overt CVD¹¹. Therefore, understanding genetic determinants of arterial stiffness and molecular mechanisms thereof, may aid in the development of novel therapies to prevent TOD and CVD.

A recent genome-wide association study (GWAS) of 9 discovery cohorts (20,634 participants; average age of cohort 34-75 years old) and 2 replication cohorts (N=5,306) identified single nucleotide polymorphisms (SNPs) in a gene desert locus on chromosome 14 with highly significant association with PWV ($p < 5.6 \times 10^{-11}$ for the top SNP, rs1381289C>T)¹². Notably, the presence of each rs1381289 allele resulted in an estimated hazard ratio = 1.05 for a first major coronary artery disease event and 1.10 for incident heart failure, suggesting that increased arterial stiffness associated with SNP variants in this locus may be causally linked to an increased risk of subsequently developing major CVD events.

The “aortic stiffness” locus spans 2 Mb between coding genes B-cell leukemia 11b (*BCL11B*) and vaccinia-related kinase 1 (*VRK1*). By performing a detailed analysis of this locus, we found an ~1.9 kb sequence, located ~850 kb downstream (3') of *BCL11B*, known to function as an enhancer for *BCL11B*¹³, but not *VRK1*. Enhancers are DNA regulatory elements that activate the expression of target genes independently of distance or orientation¹⁴. In the present study, we sought to elucidate the mechanistic basis of the association of the chromosome 14 locus with aortic stiffness and a possible cause-effect relation between BCL11B and vascular function.



BCL11B, also known as COUP-TF interacting protein-2 (CTIP2), is a transcription factor^{15,16} best known for its critical role in T cells and innate lymphoid cells^{17,18}, as well as neuronal development during embryogenesis^{19,20}; however, a role of BCL11B in the cardiovascular system has never been described. Here we report for the first time that BCL11B is expressed in the vascular smooth muscle (VSM) where it regulates vascular stiffness by increasing non-muscle actin polymerization in VSM cells via the cGMP/PKG/pVASP^{S239} signaling pathway. Notably, despite VSM *Bcl11b* deletion having profound effects on the aorta, contractile properties of resistance vessels, blood pressure and microalbuminuria in BSMKO mice remained comparable with WT mice. In contrast, we found that increased aortic stiffness in BSMKO was correlated with enhanced cerebral microbleeds compared to age-matched WT mice. Taken together, our study identifies VSM BCL11B as a novel and crucial regulator of VSM cytoskeletal assembly in large arteries affecting aortic wall stiffness and suggests that BCL11B or its downstream signaling targets are promising candidates for the translational development of therapies against arterial stiffness and related target organ microcirculatory damage.

METHODS

Data Availability.

A detailed description of Materials and Methods can be found in the online Supplemental Materials. All data and supporting material are available upon request.



RESULTS

BCL11B is expressed in VSM and is down-regulated in animal models of arterial stiffness.

A detailed analysis of the genetic locus on chromosome 14 with genome-wide association with elevated PWV¹² revealed a highly conserved 550bp sequence (> 95% homology among species) within a *BCL11B* enhancer¹³, in proximity of the highest significant SNP variant associated with increased PWV (rs1381289C>T), which has recently been shown to correlate with *BCL11B* expression²¹. By using BLAST, we identified this highly conserved 550bp sequence in a locus named AI060616 (NCBI nomenclature) and amplified one specific PCR band of expected 356 bp molecular size, confirmed by sequencing, in aortic extracts (Figure 1A).

We next sought to determine whether BCL11B, a downstream target of this genomic locus, is present in the vasculature. By using double mutant mice expressing a red fluorescent protein (mTomato) upon removal of *Bcl11b* after tamoxifen administration (*ER-Cre-Bcl11b^{lox/lox}-mTomato* mice), we were able to indirectly visualize *Bcl11b*'s localization in aortic sections and, specifically, in the tunica media (Figure 1B). These findings were confirmed by immunostaining human aortic smooth muscle cells with an antibody specific to BCL11B (Figure 1C), Western blotting of murine aortas (Figure 1D) and performing qRT-PCR of human aortas (Figure 1E). In addition to the aorta, *Bcl11b* was visualized in VSM of arteries and arterioles in heart, lung and kidney of tamoxifen-treated *ER-Cre-Bcl11b^{lox/lox}-mTomato* mice (Supplemental Figure I). Lastly, a *pGL3* luciferase reporter construct containing *Bcl11b* promoter region Chr12: 108004359-108003144 (GRCm38.p6), demonstrated that VSM cells are transcriptionally competent to sustain *Bcl11b* expression compared to an empty (control) plasmid (Figure 1F).

To determine whether *Bcl11b* expression in the vasculature was linked to arterial function, we measured *Bcl11b* in aortas of high-fat, high-sucrose (HFHS)-fed obese mice, a model of arterial stiffness we previously described^{22,23}. We found that *Bcl11b* mRNA and protein levels were significantly decreased in aortas of HFHS- compared to normal diet (ND)-fed mice (Figures 2A & 2B, quantitation

values on graphs). To further elucidate a functional role of vascular *Bcl11b* *in vivo*, we measured PWV in mice with an inducible global *Bcl11b* knock out (*ER-Cre-Bcl11b^{fllox/fllox}* treated with tamoxifen). We found that PWV was significantly increased in 10-month-old *Bcl11b* null mice compared with WT littermate controls (area under the curve: 260.3 ± 4.7 m/s*mmHg in WT vs 285.6 ± 2.8 m/s*mmHg in *Bcl11b^{-/-}*, $p=6.0 \times 10^{-3}$; over a range of mean arterial pressures, Figure 2C). Notably, PWV in *Bcl11b^{-/-}* mice increased to a similar extent as HFHS-fed obese mice (shadowed box in Figure 2C corresponding to PWV values in HFHS-fed mice, in a similar MAP range, adapted from our previous publication²²). Taken together, our novel findings demonstrate that BCL11B is present in the VSM of the aortic wall and that aortic BCL11B down-regulation may increase aortic stiffness.

VSM BCL11B regulates aortic tone and stiffness.

Based on our novel observation that BCL11B is expressed in VSM and its decreased aortic levels are associated with increased arterial stiffness, we generated mice with tamoxifen-inducible *Bcl11b* deletion in VSM (BSMKO; Supplemental Figure II). *Bcl11b* deletion in VSM did not affect gross aortic morphology, as indicated by comparable aortic media thickness (54.5 ± 1.0 μ m in WT, n=5 vs 55.1 ± 1.1 μ m in BSMKO, n=7; $p=6.9 \times 10^{-1}$) and diameters (unloaded dimensions: 0.74 ± 0.02 mm in WT, n=5 vs 0.75 ± 0.01 mm in BSMKO, n=7, $p=8.1 \times 10^{-1}$; and Supplemental Figure III for *in vivo* measurements) between WT and BSMKO mice. However, force, wall tension and stress, generated by BSMKO aortic rings (n=7) in organ baths were significantly increased compared to WT (n=5) (Figure 3A, 3B, 3C & 3D). Likewise, aortic stiffness measured by PWV *in vivo* or derived from *ex vivo* elastic modulus with the Moens-Kortweg equation, was significantly increased in BSMKO mice (n=17) 2 months after VSM *Bcl11b* removal, compared to WT littermate controls (n=14) (Figure 3E & 3F). Interestingly, aortic KCl- and phenylephrine-induced stress were not significantly affected by *Bcl11b* deletion (Figure 3G & 3H) indicating that *Bcl11b* regulates VSM force generation but not via KCl- and phenylephrine-stimulated pathways.

Bcl11b deletion in VSM did not significantly affect blood pressure or heart rate, measured by radiotelemetry in 4- or 15-month old, conscious mice over 8 consecutive days, compared to age-matched WT littermates (Online Table I). Aging comparably increased systolic and mean arterial pressures in both groups (Online Table I).

Phosphorylated VASP at serine 239 (pVASP²³⁹) is downregulated in aortas of BSMKO mice.

We used RNA sequencing to identify molecular mechanisms that may contribute to increased VSM tone and stiffness in BSMKO aortas. 458 and 329 genes were differentially up- and down-regulated, respectively, in aortic mRNA extracts of BSMKO (n=5) compared to WT (n=5) mice (Figure 4A & 4B, and Supplemental Figure IV, in which the heatmap illustrates individual levels of expression for replicate mice for each of the top 40 differentially expressed (DE) genes; $p=2.7 \times 10^{-7}$ - 3.4×10^{-4}). Pathway enrichment analysis (DAVID) on differentially expressed genes revealed that cGMP-PKG signaling pathway was the most significantly downregulated pathway in BSMKO compared to WT aortas (FDR $q=9.4 \times 10^{-3}$) (Figure 4C, and Supplemental Figures V & VI for a list of differentially regulated pathways as well as individual levels of expression for each gene within the cGMP-PKG pathway). We further validated RNA sequencing findings by analyzing levels of guanylate cyclase (GC) and cGMP-dependent protein kinase G (PKG1), the enzymes directly upstream and downstream of cGMP. We found that GC catalytic subunit isoforms ($\alpha 1$, $\alpha 2$, $\beta 1$) mRNA (Figure 4D) and PKG1 protein levels (Figure 4E, quantitation in graph) were significantly downregulated in VSM cells isolated from BSMKO aortas compared to WT. Similarly, downregulating *Bcl11b* with a validated siRNA, decreased PKG1 expression in VSM cells (Figure 4F, quantitation in graph).

As vasodilator-stimulated phosphoprotein (VASP) is a PKG1 phosphorylation target in VSM, we examined whether VASP phosphorylation was affected by *Bcl11b* deletion in VSM. Specifically, we analyzed VASP phosphorylation at serine 239, since we previously showed that VASP phosphorylation at this residue inversely correlates with arterial stiffness²³. Levels of pVASP^{S239} were dramatically decreased in BSMKO VSM cells compared to WT cells, cultured with or without FBS (Figure 5A; quantitation in graph), and in BSMKO aortas compared to WT controls (Figure 5B; quantitation in graph), while total VASP remained unchanged. Similar findings were obtained in aortas of HFHS-fed obese mice (i.e., with decreased aortic *Bcl11b*, Figure 2B), compared to ND-fed mice (Figure 5C; quantitation in graph). Our findings of decreased pVASP^{S239} were corroborated in males (n=4) and females (n=4) of a second animal model in which constitutive *Bcl11b* removal in VSM was achieved with a *Sm22α* (transgelin) promoter-driven Cre recombinase transgene (Supplemental Figure VIIA). Lastly, no statistically significant differences in pVASP^{S239} expression were observed in tamoxifen- (n=3) compared with vehicle (oil)-treated *Bcl11b*^{fl/fl} mice (n=3), excluding the possibility that tamoxifen administration *per se* may have decreased pVASP^{S239} levels in the aorta (Supplemental Figure VIIB).

In contrast to the aorta, pVASP^{S239} levels in mesenteric arteries isolated from the mesenteric plexus (Supplemental Figure VIIIA) were similar between WT (n=6) and BSMKO (n=6) mice (Supplemental Figure VIIIB). Moreover, no statistically significant differences were observed in the contractile responses to phenylephrine or vasodilation responses to papaverine of mesenteric arteries from WT (n=8) and BSMKO (n=8) (Supplemental Figure VIIIC & VIID), consistent with comparable blood pressures between WT and BSMKO mice (Online Table I). Taken together, these data suggest that the BCL11B - pVASP^{S239} axis is important for the regulation of large artery stiffness but is dispensable for vasoconstriction of resistance vessels.

In addition to protein kinases PKG and PKA²⁴, VASP phosphorylation in VSM cells is finely regulated by phosphatases (PP1, PP2A, PP2B, PP2C)²⁵ and Rho kinases (ROCK1, ROCK2). Of interest, Ca⁺⁺/calmodulin-dependent serine-threonine phosphatase calcineurin (PP2B) has been shown to directly interact with BCL11B to regulate gene expression in T-cells²⁶. Therefore, we examined whether PP2B may also contribute to decreased pVASP^{S239} levels in BSMKO VSM cells. We found that protein levels of PP2B and NFAT2, a major PP2B phosphatase target, were significantly upregulated in BSMKO VSM cells compared to WT (Figure 6A). On the contrary, expression of ROCK1, a Rho-dependent kinase involved in cytoskeletal rearrangements and an upstream VASP regulator²⁷, was not significantly affected by *Bcl11b* deletion (Supplemental Figure VIIC). Furthermore, overnight treatment with two PP2B inhibitors, cyclosporine A (1-10μM) or the more specific PP2B inhibitor calcineurin autoinhibitory peptide (CAIP, 10-100μM), restored pVASP^{S239} towards control levels in BSMKO VSM cells in a dose-dependent manner (Figures 6B & 6C; quantitation in graph), indicating that decreased pVASP^{S239} in BSMKO VSM is dependent, at least in part, on increased PP2B activity. Lastly, overexpressing *Bcl11b* in aortic media rings by transient transfection for 3 days was sufficient to significantly restore PKG, pVASP^{S239} and decrease PP2B to control levels (Figure 6D).

Actin polymerization is dependent on VASP phosphorylation in VSM Bcl11b deleted aortas.

VASP is an important regulator of non-muscle actin polymerization-dependent VSM tone²⁸ whereas phosphorylation of VASP at serine 239 (pVASP^{S239}) inhibits actin polymerization in VSM cells²⁹, thereby regulating cytoskeletal actin assembly. We found increased filamentous to globular (F/G) actin ratio, indicative of increased actin polymerization, in BSMKO aortas compared to WT (Figure 7A). Moreover, α-actinin, a major VASP-interacting protein during actin polymerization, was significantly upregulated in BSMKO (n=4) compared to WT (n=4) aortas (Figure 7B, quantitation in graph). Notably, pre-incubation with the specific PP2B inhibitor CAIP (10μM, 1 hr, 37°C), decreased both F/G actin ratio (Figure 7C) and aortic stiffness (from 245.7 ± 4.3 kPa in BSMKO, n=4, to 184.0 ± 17.2 kPa in BSMKO/CAIP, n=4; *p*=3.0×10⁻²; Figure 7D) in BSMKO aortic rings. Taken together, our data indicate

that lack of VSM BCL11B increases aortic stiffness, at least in part, because of decreased pVASP^{S239} levels and associated increased actin polymerization.

VSM Bcl11b deletion increased the incidence of cerebral microbleeds.

Emerging evidence strongly correlates measures of arterial stiffness (PWV and increased pulse pressure) with microcirculatory end-organ damage, including kidney disease^{30,31} and cognitive impairment³²⁻³⁴. We sought to determine whether increased aortic stiffness in BSMKO mice is associated with increased indexes of end-organ microcirculatory injury (microalbuminuria, cerebral microbleeds and retinal vessel density). We found that the urinary albumin to creatinine ratio was not significantly affected by VSM *Bcl11b* deletion compared to WT littermates (23.2 ± 5.6 $\mu\text{g}/\text{mg}$ in WT, $n=12$, and 12.0 ± 5.3 $\mu\text{g}/\text{mg}$ in BSMKO, $n=8$; $p=1.9 \times 10^{-1}$; Supplemental Figure IXA). In contrast, a significantly higher number of cerebral microbleeds was identified by magnetic resonance imaging mainly in the thalamus of BSMKO compared to WT mice (1.0 ± 0.4 in WT, $n=5$, vs 6.5 ± 1.7 in BSMKO, $n=6$; $p=1.0 \times 10^{-2}$) (Figure 8A). Histological staining of brain sections with Prussian blue confirmed an increased number of cerebral microbleeds in BSMKO compared to WT mice ($5.7 \pm 1.0 \times 10^3$ μm^2 in WT, $n=12$, vs $11.2 \pm 2.2 \times 10^3$ μm^2 in BSMKO, $n=12$; $p=3.0 \times 10^{-2}$) (Figure 8B). Interestingly, cerebral microbleeds in BSMKO mice were comparable to HFHS-fed mice, in which we similarly observed significant increases in cerebral microbleeds compared to ND-fed control mice ($7.0 \pm 1.4 \times 10^3$ μm^2 in ND, $n=6$, vs $12.6 \pm 2.2 \times 10^3$ μm^2 in HFHS, $n=6$; $p=5.0 \times 10^{-2}$) (Figure 8C). No statistically significant differences were observed between aged WT and BSMKO (24-months old) ($13.8 \pm 4.2 \times 10^3$ μm^2 in WT, $n=4$, vs $12.0 \pm 8.0 \times 10^3$ μm^2 in BSMKO, $n=4$; $p=3.9 \times 10^{-1}$), indicating that VSM *Bcl11b* deletion accelerated the development of aging-associated cerebral microbleeds, which then plateaued to levels comparable to aged WT. Independently of the presence of cerebral microbleeds, no statistically significant difference in cognitive function was detected between 5-month or 24-month old WT and BSMKO mice as assessed by a novel object recognition test (Supplemental Figure IXB).

Consistent with cerebral microvascular damage, total and average vessel length and branching, measured in isolectin B4-stained retinal flat-mounts, trended to increase in BSMKO compared to WT as well as in HFHS-fed compared to ND-fed mice (Supplemental Figure IXC), suggesting a stimulation of neovessel growth in a damaged retinal microvasculature.

DISCUSSION

Arterial stiffness, or loss of elastic compliance of large arteries, is a strong, independent risk factor for cardiovascular diseases (CVD)^{2,6}. Elevated pulse wave velocity (PWV), the gold standard measure of aortic wall stiffness, strongly associates with adverse cardiovascular outcomes⁶⁻⁸. Moreover, mounting evidence correlates measures of arterial stiffness and pressure pulsatility (PWV, pulse pressure) to kidney disease^{30,31} and cognitive impairment/dementia^{32,34}. However, genetic and molecular cues of aortic wall stiffening are not fully understood hampering the discovery of therapeutic targets that can slow or reverse arterial stiffening thereby decreasing target organ damage and the risk of developing overt CVD.

Arterial stiffness trait loci are moderately heritable³⁵ but little is known about genetic determinants of arterial stiffness. A recent genome-wide association study (GWAS) demonstrated that SNPs in the vicinity of the *BCL11B* genetic locus are associated with increased arterial stiffness and subsequent risk of developing CVD¹². Interestingly, the most significant SNP variant (rs1381289 C>T) in this “aortic stiffness” locus falls in a highly conserved sequence within a *BCL11B* enhancer. We postulated that SNP variants in the 3’-*BCL11B* locus may alter the *BCL11B* gene enhancer function and

may play a causal role in the pathogenesis of arterial stiffness by regulating *BCL11B* expression. A recent report showed that rs1381289 C>T genotype in the 3'-*BCL11B* locus inversely correlates with *BCL11B* mRNA expression in aortic rings from transplant donors²¹, despite the authors not detecting any *BCL11B* protein expression in the same aortic rings. These observations prompted us to further examine whether *BCL11B* is present in the vasculature and whether there is a cause-effect relation between *BCL11B* and vascular function.

Our novel findings demonstrate that *BCL11B*, previously known solely for its role in T lymphocyte³⁶ and neuronal¹⁹ lineage commitment, is expressed in the VSM of the aortic wall. Importantly, here we report for the first time that VSM *BCL11B* is a crucial regulator of VSM structural components and aortic stiffness, as corroborated by the following findings: (1) *in vivo Bcl11b* deletion in VSM (BSMKO mice) resulted in increased non-muscle actin polymerization (F/G actin ratio); (2) mice lacking *Bcl11b* globally or specifically in VSM (BSMKO) have increased PWV, the *in vivo* index of arterial stiffness, compared to WT littermates; (3) aortic rings from BSMKO mice have increased force, stress, wall tension and stiffness compared to WT; and (4) *Bcl11b* is downregulated in aortas of high fat, high sucrose-fed obese mice, a mouse model of arterial stiffness that we previously described²². Although a major *BCL11B* interacting protein, COUP-TFII, has been previously shown to partake in atria and blood vessel development during embryogenesis³⁷, to the best of our knowledge, this is the first report of a functional role of *BCL11B* in the adult cardiovascular system.

Furthermore, we uncovered a pivotal role of VSM *BCL11B* in the regulation of VSM cytoskeletal filaments, which form a coordinated system to efficiently transduce contractile forces to the extracellular matrix and among adjacent VSM cells, thereby sustaining aortic wall mechanics and compliance. In response to pressure or mechanical stretch, thin filament dynamic assembly, namely non-muscle actin polymerization, become a major determinant of VSM contraction and basal tone^{38,39}, independently of myosin light chain 2 phosphorylation and actino-myosin cross-bridges cycles^{40,41}. Cytoskeletal actin polymerization can sustain VSM force generation and cytoskeletal stiffness to maintain vessel diameter in response to wall tension or stretch⁴², as it may occur in the aorta exposed to cyclic strain induced by cardiac contraction, particularly in the proximal regions. Therefore, our finding of increased filamentous/globular (F/G) actin ratio, indicative of increased actin polymerization, is consistent with increased force and wall tension in BSMKO aortas and increased PWV in BSMKO mice compared to WT controls.

At the molecular level, we found that the cGMP/PKG/ pVASP^{S239} signaling pathway was dramatically decreased in BSMKO aortas and VSM cells, while total VASP remained unchanged. VASP has emerged as an important mediator of actin polymerization-dependent VSM force generation. Specifically, VASP interacts with α -actinin, vinculin, zyxin and other components of thin filament assembly at focal adhesion and dense bodies, which are important sites of VSM contractile filament attachment, cell-cell interactions and cell adhesion to the extracellular matrix, thereby contributing to VSM tone and stiffness independently of myosin light chain 2 phosphorylation^{28,43-45}. The drug cytochalasin D, commonly used to block actin polymerization in a variety of cell types, is known to interfere with VASP localization to nascent F-actin filaments⁴⁶ underscoring the pivotal role of VASP in cytoskeletal actin rearrangement. Moreover, VASP overexpression has been shown to induce F-actin assembly⁴⁷; in contrast, VASP phosphorylation at serine 239 is sufficient to inhibit actin filament polymerization²⁹. Interestingly, we found that partially restoring decreased pVASP^{S239} with a calcineurin inhibitor was able to reverse the increased actin polymerization and aortic stiffness in BSMKO aortic rings towards normal levels. Overall, our results suggest that cyclosporinA or specific PP2B inhibitors as well as compounds that inhibit actin filament assembly may become potential pharmacological candidates for arterial stiffness.

Interestingly, despite having profound effects on the aorta, lack of VSM *Bcl11b* did not affect pVASP^{S239} levels and contractile properties of resistance arteries, nor blood pressure in BSMKO mice suggesting a dispensable role of BCL11B in the regulation of VSM tone in resistance vessels. This intriguing finding on a differential role of BCL11B in VSM of large *versus* small arteries could be explained by the fact that smooth muscle along the adult vascular tree is not homogeneous but rather a mosaic of phenotypically and functionally distinct smooth muscle cell types⁴⁸. Elegant lineage mapping studies have demonstrated that smooth muscle of proximal regions of the aorta, which are the most susceptible to vascular stiffening, namely the outflow tract, innominate, carotid and subclavian arteries, but not the smooth muscle of resistance vessels, developmentally originates from the cranial neural crest⁴⁹. Considering that BCL11B is highly expressed and required for neuronal development during embryogenesis^{19,20}, BCL11B may be a regulator of VSM-specific gene programs of neural crest-derived proximal, but not distal, vascular regions. Further studies are warranted to fully elucidate the role of BCL11B in the development of the cardiovascular system during embryogenesis.

Arterial stiffness markedly increases the risk of adverse cardiovascular outcomes^{6,7,50} including heart failure^{51,52}, coronary artery disease⁹ and hypertension^{3,4}. In addition, emerging evidence correlates measures of arterial stiffness (PWV and pulse pressure) with cognitive decline^{32,34} and kidney disease^{30,31}. Elastic compliance of large arteries is paramount to dampen the pulsatility of cardiac contraction and to ensure a steady blood supply to peripheral organs while limiting the pulsatile energy that penetrates into the microcirculation. However, as the aortic wall stiffens with age and obesity⁵³, this buffering effect is lost, thereby increasing the amount of pressure and flow pulsatility transmitted to the downstream microcirculation, where it triggers microvascular remodeling, impaired reactivity and abnormal flow autoregulation^{54,55}. Of clinical importance, this microcirculatory injury may lead to structural and functional changes generally referred to as target organ damage, particularly in high flow/low resistance organs, such as brain and kidneys. An interesting finding of our study is that mice lacking *Bcl11b* in the VSM, with elevated arterial stiffness, have a significant increase in cerebral microbleeds compared to age-matched WT controls. Thalamus and hippocampus were the brain regions mostly affected - a finding consistent with epidemiological studies reporting that white matter hyperintensities and consequent cognitive decline and dementia associated with arterial stiffness are generally observed in deep central regions of the brain, which are particularly sensitive to pulsatile stress transmitted via branches of the carotid arteries penetrating the deep parenchyma^{56,57}. Although further studies are warranted to assess the effect of VSM *Bcl11b* deletion on the cerebral microvasculature, lack of BCL11B in VSM did not affect blood pressure or microalbuminuria in BSMKO mice compared to age-matched WT controls, consistent with the cerebral microcirculation being particularly sensitive to excessive pressure pulsatility triggered by arterial stiffness in the absence of VSM *Bcl11b* compared to renal or other resistive vessel beds.

In conclusion, our study has uncovered a novel and crucial role for VSM BCL11B in aortic structural and functional integrity and strongly supports BCL11B or its downstream regulated pathways as potential therapeutic targets against arterial stiffness (illustrated in the graphic summary). Although, the cause-effect relationship as well as the temporal progression from arterial stiffness to target organ damage, including hypertension, remains to be fully unraveled, as we previously pointed out⁵⁸, targeting arterial stiffness could represent a novel clinical approach to prevent the progression into target organ damage leading to cardiovascular complications and cognitive decline. Further studies in human populations from different ethnic groups are warranted to establish whether the genotype at the 3'-*BCL11B* locus may be used as diagnostic biomarker to identify individuals at increased risk of developing arterial stiffness and other vascular diseases.

ACKNOWLEDGEMENTS

We would like to thank the Boston University Medical Campus Analytical Instrumentation, Cellular Imaging and MRI/NMR High Field Imaging Cores for the expert technical support.

AUTHORS CONTRIBUTIONS

JAV, JM, LV, EB, JBG, CJN, KS performed experiments, contributed to study design, data interpretation and reviewed the manuscript; EYH analyzed RNA sequencing datasets; DA provided *Bcl11b^{flx/flx}* mouse strain used in the study; RAC, DA, GFM, KGM provided critical comments to the study and the manuscript; FS contributed to the study design, coordinated the study, designed and performed experiments, analyzed and interpreted the data and wrote the manuscript.

DISCLOSURES

GFM is the owner of Cardiovascular Engineering Inc., a manufacturer of biomedical devices for arterial stiffness measurements.

SOURCES OF FUNDING

This work has been possible thanks to the financial support of NIH grants HL136311 to FS; HL105287 to RAC; AG053274, AG050599 and HL136224 to KGM; AI067846 to DA; NHLBI's Framingham Heart Study Contracts No. N01-HC-25195 and HHSN268201500001I and grants HL070100, HL080124, HL107385 and HL126136 to GFM; NIH T32 training grant HL007224 to JM and JBG; pilot grants 1UL1TR001430 and 5P30DK046200 to FS and by the Evans Center for Interdisciplinary Biomedical Research Arterial Stiffness ARC at Boston University (<http://www.bumc.bu.edu/evanscenteribr/>).

 American Heart Association.

SUPPLEMENTAL MATERIALS

Expanded Materials & Methods

Major Resources Table

Supplemental Figures I-XI

Online Table I

References 59-71

Circulation
Research

REFERENCES

1. Virani SS, Alonso A, Benjamin EJ, Bittencourt MS, Callaway CW, Carson AP, Chamberlain AM, Chang AR, Cheng S, Delling FN, et al. Heart disease and stroke statistics—2020 update: A report from the American Heart Association. *Circulation*. 2020.
2. Willum-Hansen T, Staessen JA, Torp-Pedersen C, Rasmussen S, Thijs L, Ibsen H, Jeppesen J. Prognostic value of aortic pulse wave velocity as index of arterial stiffness in the general population. *Circulation*. 2006;113(5):664–670.
3. Kaess BM, Rong J, Larson MG, Hamburg NM, Vita JA, Levy D, Benjamin EJ, Vasan RS, Mitchell GF. Aortic Stiffness, Blood Pressure Progression, and Incident Hypertension. *JAMA*. 2012;308(9):875.
4. Najjar SS, Scuteri A, Shetty V, Wright JG, Muller DC, Fleg JL, Spurgeon HP, Ferrucci L, Lakatta EG. Pulse wave velocity is an independent predictor of the longitudinal increase in systolic blood pressure and of incident hypertension in the Baltimore Longitudinal Study of Aging. *J Am Coll Cardiol*. 2008;51(14):1377–1383.
5. AlGhatrif M, Strait JB, Morrell CH, Canepa M, Wright J, Elango P, Scuteri A, Najjar SS, Ferrucci L, Lakatta EG. Longitudinal Trajectories of Arterial Stiffness and the Role of Blood Pressure: The Baltimore Longitudinal Study of Aging. *Hypertension*. 2013;62(5):934–941.
6. Mitchell GF, Hwang SJ, Vasan RS, Larson MG, Pencina MJ, Hamburg NM, Vita JA, Levy D, Benjamin EJ. Arterial stiffness and cardiovascular events: the Framingham Heart Study.

- Circulation*. 2010;121(4):505–511.
7. Sutton-Tyrrell K, Najjar SS, Boudreau RM, Venkitachalam L, Kupelian V, Simonsick EM, Havlik R, Lakatta EG, Spurgeon H, Kritchevsky S, et al. Elevated aortic pulse wave velocity, a marker of arterial stiffness, predicts cardiovascular events in well-functioning older adults. *Circulation*. 2005;111(25):3384–3390.
 8. Vlachopoulos C, Aznaouridis K, Stefanadis C. Prediction of cardiovascular events and all-cause mortality with arterial stiffness: a systematic review and meta-analysis. *J Am Coll Cardiol*. 2010;55(13):1318–1327.
 9. Mattace-Raso FU, van der Cammen TJ, Hofman A, van Popele NM, Bos ML, Schalekamp MA, Asmar R, Reneman RS, Hoeks AP, Breteler MM, et al. Arterial stiffness and risk of coronary heart disease and stroke: the Rotterdam Study. *Circulation*. 2006;113(5):657–663.
 10. Ding J, Mitchell GF, Bots ML, Sigurdsson S, Harris TB, Garcia M, Eiriksdottir G, van Buchem MA, Gudnason V, Launer LJ. Carotid Arterial Stiffness and Risk of Incident Cerebral Microbleeds in Older People. *Arteriosclerosis, Thrombosis, and Vascular Biology*. 2015;35(8):1889–1895.
 11. Williams B, Mancia G, Spiering W, Agabiti Rosei E, Azizi M, Burnier M, Clement DL, Coca A, de Simone G, Dominiczak A, et al. 2018 ESC/ESH Guidelines for the management of arterial hypertension. *European Heart Journal*. 2018;39(33):3021–3104.
 12. Mitchell GF, Verwoert GC, Tarasov K V, Isaacs A, Smith A V, Yasmin, Rietzschel ER, Tanaka T, Liu Y, Parsa A, et al. Common genetic variation in the 3'-BCL11B gene desert is associated with carotid-femoral pulse wave velocity and excess cardiovascular disease risk: the AortaGen Consortium. *Circ Cardiovasc Genet*. 2012;5(1):81–90.
 13. Li L, Zhang JA, Dose M, Kueh HY, Mosadeghi R, Gounari F, Rothenberg E V. A far downstream enhancer for murine Bcl11b controls its T-cell specific expression. *Blood*. 2013;122(6):902–911.
 14. Natoli G, Andrau JC. Noncoding transcription at enhancers: general principles and functional models. *Annu Rev Genet*. 2012;46:1–19.
 15. Avram D, Fields A, Senawong T, Topark-Ngarm A, Leid M. COUP-TF (chicken ovalbumin upstream promoter transcription factor)-interacting protein 1 (CTIP1) is a sequence-specific DNA binding protein. *Biochem J*. 2002;368(Pt 2):555–563.
 16. Avram D, Fields A, Pretty On Top K, Nevriy DJ, Ishmael JE, Leid M. Isolation of a novel family of C(2)H(2) zinc finger proteins implicated in transcriptional repression mediated by chicken ovalbumin upstream promoter transcription factor (COUP-TF) orphan nuclear receptors. *J Biol Chem*. 2000;275(14):10315–10322.
 17. Avram D, Califano D. The Multifaceted Roles of Bcl11b in Thymic and Peripheral T Cells: Impact on Immune Diseases. *The Journal of Immunology*. 2014;193(5):2059–2065.
 18. Califano D, Cho JJ, Uddin MN, Lorentsen KJ, Yang Q, Bhandoola A, Li H, Avram D. Transcription Factor Bcl11b Controls Identity and Function of Mature Type 2 Innate Lymphoid Cells. *Immunity*. 2015;43(2):354–368.
 19. Srinivasan K, Leone DP, Bateson RK, Dobrova G, Kohwi Y, Kohwi-Shigematsu T, Grosschedl R, McConnell SK. A network of genetic repression and derepression specifies projection fates in the developing neocortex. *Proc Natl Acad Sci U S A*. 2012;109(47):19071–19078.
 20. Simon R, Brylka H, Schwegler H, Venkataramanappa S, Andratschke J, Wiegrefe C, Liu P, Fuchs E, Jenkins NA, Copeland NG, et al. A dual function of Bcl11b/Ctip2 in hippocampal neurogenesis. *EMBO J*. 2012;31(13):2922–2936.
 21. Maskari R Al, Hardege I, Cleary S, Figg N, Li Y, Siew K, Khir A, Yu Y, Liu P, Wilkinson I, et al. Functional characterization of common BCL11B gene desert variants suggests a lymphocyte-mediated association of BCL11B with aortic stiffness. *European Journal of Human Genetics*. 2018.
 22. Weisbrod RM, Shiang T, Al Sayah L, Fry JL, Bajpai S, Reinhart-King CA, Lob HE, Santhanam L, Mitchell G, Cohen RA, et al. Arterial Stiffening Precedes Systolic Hypertension in Diet-Induced Obesity. *Hypertension*. 2013;62(6):1105–1110.

23. Fry JL, Al Sayah L, Weisbrod RM, Van Roy I, Weng X, Cohen RA, Bachschmid MM, Seta F. Vascular Smooth Muscle Sirtuin-1 Protects Against Diet-Induced Aortic Stiffness. *Hypertension*. 2016;68(3):775–784.
24. Butt E, Abel K, Krieger M, Palm D, Hoppe V, Hoppe J, Walter U. cAMP- and cGMP-dependent protein kinase phosphorylation sites of the focal adhesion vasodilator-stimulated phosphoprotein (VASP) in vitro and in intact human platelets. *The Journal of biological chemistry*. 1994;269(20):14509–17.
25. Abel K, Mieskes G, Walter U. Dephosphorylation of the focal adhesion protein VASP in vitro and in intact human platelets. *FEBS letters*. 1995;370(3):184–8.
26. Tosello V, Saccomani V, Yu J, Bordin F, Amadori A, Piovan E. Calcineurin complex isolated from T-cell acute lymphoblastic leukemia (T-ALL) cells identifies new signaling pathways including mTOR/AKT/S6K whose inhibition synergize with calcineurin inhibition to promote T-ALL cell death. *Oncotarget*. 2016;7(29):45715–45729.
27. Döppler H, Storz P. Regulation of VASP by phosphorylation. *Cell Adhesion & Migration*. 2013;7(6):492–496.
28. Kim HR, Graceffa P, Ferron F, Gallant C, Boczkowska M, Dominguez R, Morgan KG. Actin polymerization in differentiated vascular smooth muscle cells requires vasodilator-stimulated phosphoprotein. *AJP: Cell Physiology*. 2010;298(3):C559–C571.
29. Benz PM, Blume C, Seifert S, Wilhelm S, Waschke J, Schuh K, Gertler F, Munzel T, Renne T. Differential VASP phosphorylation controls remodeling of the actin cytoskeleton. *Journal of Cell Science*. 2009;122(21):3954–3965.
30. Woodard T, Sigurdsson S, Gotal JD, Torjesen AA, Inker LA, Aspelund T, Eiriksdottir G, Gudnason V, Harris TB, Launer LJ, et al. Mediation Analysis of Aortic Stiffness and Renal Microvascular Function. *Journal of the American Society of Nephrology*. 2015;26(5):1181–1187.
31. Moody WE, Edwards NC, Chue CD, Ferro CJ, Townend JN. Arterial disease in chronic kidney disease. *Heart*. 2013;99(6):365–372.
32. Ding J, Mitchell GF, Bots ML, Sigurdsson S, Harris TB, Garcia M, Eiriksdottir G, van Buchem MA, Gudnason V, Launer LJ. Carotid arterial stiffness and risk of incident cerebral microbleeds in older people: the Age, Gene/Environment Susceptibility (AGES)-Reykjavik study. *Arteriosclerosis, thrombosis, and vascular biology*. 2015;35(8):1889–95.
33. M.L. M, P. P, H. T, J.A. D, J. W, C. J, D. K, M. G, T.H. M. Association of arterial stiffness and pressure amplification with mild cognitive impairment and dementia: The atherosclerosis risk in communities study-neurocognitive study (ARIC-NCS). *Circulation*. 2016.
34. Cooper LL, Woodard T, Sigurdsson S, Van Buchem MA, Torjesen AA, Inker LA, Aspelund T, Eiriksdottir G, Harris TB, Gudnason V, et al. Cerebrovascular Damage Mediates Relations Between Aortic Stiffness and Memory. *Hypertension*. 2016.
35. Mitchell GF, DeStefano AL, Larson MG, Benjamin EJ, Chen MH, Vasani RS, Vita JA, Levy D. Heritability and a genome-wide linkage scan for arterial stiffness, wave reflection, and mean arterial pressure: the Framingham Heart Study. *Circulation*. 2005;112(2):194–199.
36. Wakabayashi Y, Watanabe H, Inoue J, Takeda N, Sakata J, Mishima Y, Hitomi J, Yamamoto T, Utsuyama M, Niwa O, et al. Bcl11b is required for differentiation and survival of alphabeta T lymphocytes. *Nat Immunol*. 2003;4(6):533–539.
37. Wu SP, Cheng CM, Lanz RB, Wang T, Respress JL, Ather S, Chen W, Tsai SJ, Wehrens XH, Tsai MJ, et al. Atrial identity is determined by a COUP-TFII regulatory network. *Dev Cell*. 2013;25(4):417–426.
38. Davis MJ, Wu X, Nurkiewicz TR, Kawasaki J, Davis GE, Hill MA, Meininger GA. Integrins and mechanotransduction of the vascular myogenic response. *American journal of physiology. Heart and circulatory physiology*. 2001;280(4):H1427–33.
39. Wang N, Butler JP, Ingber DE. Mechanotransduction across the cell surface and through the cytoskeleton. *Science (New York, N.Y.)*. 1993;260(5111):1124–7.
40. Chatterjee M, Murphy RA. Calcium-dependent stress maintenance without myosin

- phosphorylation in skinned smooth muscle. *Science (New York, N.Y.)*. 1983;221(4609):464–6.
41. Dillon PF, Aksoy MO, Driska SP, Murphy RA. Myosin phosphorylation and the cross-bridge cycle in arterial smooth muscle. *Science (New York, N.Y.)*. 1981;211(4481):495–7.
 42. Cipolla MJ, Gokina NI, Osol G. Pressure-induced actin polymerization in vascular smooth muscle as a mechanism underlying myogenic behavior. *FASEB journal: official publication of the Federation of American Societies for Experimental Biology*. 2002;16(1):72–6.
 43. Krause M, Dent EW, Bear JE, Loureiro JJ, Gertler FB. Ena/VASP proteins: regulators of the actin cytoskeleton and cell migration. *Annual review of cell and developmental biology*. 2003;19(1):541–64.
 44. Reinhard M, Giehl K, Abel K, Haffner C, Jarchau T, Hoppe V, Jockusch BM, Walter U. The proline-rich focal adhesion and microfilament protein VASP is a ligand for profilins. *The EMBO journal*. 1995;14(8):1583–9.
 45. Reinhard M, Jouvenal K, Tripier D, Walter U. Identification, purification, and characterization of a zyxin-related protein that binds the focal adhesion and microfilament protein VASP (vasodilator-stimulated phosphoprotein). *Proceedings of the National Academy of Sciences of the United States of America*. 1995;92(17):7956–60.
 46. Bear JE, Svitkina TM, Krause M, Schafer DA, Loureiro JJ, Strasser GA, Maly I V, Chaga OY, Cooper JA, Borisy GG, et al. Antagonism between Ena/VASP proteins and actin filament capping regulates fibroblast motility. *Cell*. 2002;109(4):509–21.
 47. Grosse R, Copeland JW, Newsome TP, Way M, Treisman R. A role for VASP in RhoA-Diaphanous signalling to actin dynamics and SRF activity. *The EMBO journal*. 2003;22(12):3050–61.
 48. Majesky MW. Developmental basis of vascular smooth muscle diversity. *Arteriosclerosis, thrombosis, and vascular biology*. 2007;27(6):1248–58.
 49. Jiang X, Rowitch DH, Soriano P, McMahon AP, Sucov HM. Fate of the mammalian cardiac neural crest. *Development*. 2000;127(8):1607–1616.
 50. Vlachopoulos C, Aznaouridis K, O'Rourke MF, Safar ME, Baou K, Stefanadis C. Prediction of cardiovascular events and all-cause mortality with central haemodynamics: a systematic review and meta-analysis. *Eur Heart J*. 2010;31(15):1865–1871.
 51. Kaess BM, Rong J, Larson MG, Hamburg NM, Vita JA, Cheng S, Aragam J, Levy D, Benjamin EJ, Vasani RS, et al. Relations of Central Hemodynamics and Aortic Stiffness with Left Ventricular Structure and Function: The Framingham Heart Study. *Journal of the American Heart Association*. 2016;5(3).
 52. Bell V, McCabe EL, Larson MG, Rong J, Merz AA, Osypiuk E, Lehman BT, Stantchev P, Aragam J, Benjamin EJ, et al. Relations between aortic stiffness and left ventricular mechanical function in the community. *Journal of the American Heart Association*. 2017.
 53. Sutton-Tyrrell K, Newman A, Simonsick EM, Havlik R, Pahor M, Lakatta E, Spurgeon H, Vaitkevicius P. Aortic stiffness is associated with visceral adiposity in older adults enrolled in the study of health, aging, and body composition. *Hypertension*. 2001;38(3):429–433.
 54. Mitchell GF. Effects of central arterial aging on the structure and function of the peripheral vasculature: implications for end-organ damage. *Journal of Applied Physiology*. 2008;105(5):1652–1660.
 55. Cooper LL, Palmisano JN, Benjamin EJ, Larson MG, Vasani RS, Mitchell GF, Hamburg NM. Microvascular function contributes to the relation between aortic stiffness and cardiovascular events. *Circulation: Cardiovascular Imaging*. 2016.
 56. Van Den Bergh R. Centrifugal elements in the vascular pattern of the deep intracerebral blood supply. *Angiology*. 1969.
 57. Mitchell GF, van Buchem MA, Sigurdsson S, Gotal JD, Jonsdottir MK, Kjartansson Ó, Garcia M, Aspelund T, Harris TB, Gudnason V, et al. Arterial stiffness, pressure and flow pulsatility and brain structure and function: the Age, Gene/Environment Susceptibility – Reykjavik Study. *Brain*. 2011;134(11):3398–3407.



58. Oh YS, Berkowitz DE, Cohen RA, Figueroa CA, Harrison DG, Humphrey JD, Larson DF, Leopold JA, Mecham RP, Ruiz-Opazo N, et al. A Special Report on the NHLBI Initiative to Study Cellular and Molecular Mechanisms of Arterial Stiffness and Its Association With Hypertension. *Circulation research*. 2017;121(11):1216–1218.
59. Li P, Burke S, Wang J, Chen X, Ortiz M, Lee SC, Lu D, Campos L, Goulding D, Ng BL, et al. Reprogramming of T cells to natural killer-like cells upon Bcl11b deletion. *Science*. 2010.
60. Fry JL, Shiraishi Y, Turcotte R, Yu X, Gao YZ, Akiki R, Bachschmid M, Zhang Y, Morgan KG, Cohen RA, et al. Vascular Smooth Muscle Sirtuin-1 Protects Against Aortic Dissection During Angiotensin II-Induced Hypertension. *Journal of the American Heart Association*. 2015;4(9):e002384.
61. Nicholson CJ, Seta F, Lee S, Morgan KG. MicroRNA-203 mimics age-related aortic smooth muscle dysfunction of cytoskeletal pathways. *Journal of Cellular and Molecular Medicine*. 2017;21(1):81–95.
62. Qin Z, Hou X, Weisbrod RM, Seta F, Cohen RA, Tong X. Nox2 mediates high fat high sucrose diet-induced nitric oxide dysfunction and inflammation in aortic smooth muscle cells. *Journal of Molecular and Cellular Cardiology*. 2014;72:56–63.
63. O'Rourke M. Arterial stiffness, systolic blood pressure, and logical treatment of arterial hypertension. *Hypertension*. 1990;15(4):339–347.
64. Saphirstein RJ, Gao YZ, Lin QQ, Morgan KG. Cortical actin regulation modulates vascular contractility and compliance in veins. *J Physiol*. 2015;593(17):3929–3941.
65. Gao YZ, Saphirstein RJ, Yamin R, Suki B, Morgan KG. Aging impairs smooth muscle-mediated regulation of aortic stiffness: a defect in shock absorption function? *Am J Physiol Heart Circ Physiol*. 2014;307(8):H1252-61.
66. Lorentsen KJ, Cho JJ, Luo X, Zuniga AN, Urban JF, Zhou L, Gharaibeh R, Jobin C, Kladde MP, Avram D. Bcl11b is essential for licensing Th2 differentiation during helminth infection and allergic asthma. *Nature Communications*. 2018.
67. Kim HR, Gallant C, Leavis PC, Gunst SJ, Morgan KG. Cytoskeletal remodeling in differentiated vascular smooth muscle is actin isoform dependent and stimulus dependent. *Am J Physiol Cell Physiol*. 2008;295(3):C768-78.
68. Greenberg SM, Vernooij MW, Cordonnier C, Viswanathan A, Al-Shahi Salman R, Warach S, Launer LJ, Van Buchem MA, Breteler MM. Cerebral microbleeds: a guide to detection and interpretation. *The Lancet Neurology*. 2009.
69. Zudaire E, Gambardella L, Kurcz C, Vermeren S. A computational tool for quantitative analysis of vascular networks. *PLoS ONE*. 2011.
70. Leger M, Quiedeville A, Bouet V, Haelewyn B, Boulouard M, Schumann-Bard P, Freret T. Object recognition test in mice. *Nature Protocols*. 2013.
71. Pérez-Escudero A, Vicente-Page J, Hinz RC, Arganda S, De Polavieja GG. IdTracker: Tracking individuals in a group by automatic identification of unmarked animals. *Nature Methods*. 2014.

FIGURE LEGENDS

Figure 1. BCL11B is expressed in vascular smooth muscle (VSM). (A) A conserved region within the 3'-*BCL11B* genetic locus with SNPs highly associated with arterial stiffness is present in murine aortas and identified as AI060616 (NCBI). AI060616 356bp nucleotide sequence was confirmed by sequencing PCR products from aortic DNA obtained from two C57Bl/6J mice (1 and 2). Sequencing chromatogram tracing shown in lower panel. (B) Representative fluorescent images of aortic sections, taken at 20X and 40X magnification, indicating Bcl11b's localization in VSM. Red fluorescence indicates Tomato (mT) expression in lieu of Bcl11b, upon tamoxifen-induced *Bcl11b* removal and mT induction in three *ER-Cre-Bcl11b^{fllox/fllox}-mTomato* mice. Asterisks indicate clusters of VSM cells with high mT fluorescence intensity. (C) Representative images (40X magnification) of human primary aortic smooth muscle cell immunostaining with anti-BCL11B; rabbit IgG serves as negative control for antibody specificity. DAPI indicates nuclei. n=3 replicates with 3 different cell lines, as described in Materials & Methods. (D) Western blot on murine aortas confirmed Bcl11b protein expression, with a band of expected MW 100-120kDa. β -actin serves as loading control. Each lane represents one mouse. (E) Image of 1% agarose gel electrophoresis of qRT-PCR Taqman products indicates *BCL11B* mRNA expression in human aortas (n=9). Each lane represents one human subject. β -ACTIN used as endogenous housekeeping gene in multiplexed assay. (F) Relative luciferase activity (RLA), expressed as a ratio with *Renilla* luciferase, in VSM cells transfected with luciferase reporter plasmids expressing an empty plasmid (*pGL3*) or *Bcl11b* promoter (*pGL3-pr3*). Results represent 3 replicate experiments. *, $p=2.0 \times 10^{-2}$ by unpaired t-test.

Figure 2. BCL11B downregulation is associated with increased arterial stiffness. (A) *Bcl11b* mRNA levels measured by quantitative RT-PCR ($2^{-\Delta\Delta C_t}$) are decreased in aortas of HFHS-fed obese mice (ND; normal diet; HFHS, high fat, high sucrose diet), a model of arterial stiffness, compared to ND-fed mice. n=4 mice in each group; *, $p=3.0 \times 10^{-2}$ by Mann-Whitney non-parametric test. (B) Representative Western Blot of Bcl11b protein expression in aortic homogenates of ND- and HFHS-fed mice. Each lane represents one mouse. GAPDH serves as loading control. Bar graph summarizes protein band quantitation (ratio of Bcl11b over GAPDH band intensities), each dot represents one mouse. n=6 mice in each group; *, $p=1.0 \times 10^{-2}$ by unpaired t-test. (C) Pulse wave velocity (PWV, m/s), the *in vivo* index of arterial stiffness, measured over a range of mean arterial pressures (MAP, mmHg), is increased in 10-month old mice lacking *Bcl11b* compared to WT littermates. n=4 mice in each group; area under the curve (AUC): 260.3 ± 4.7 m/s*mmHg in WT vs 285.6 ± 2.8 m/s*mmHg in *Bcl11b^{-/-}*; *, $p=6.0 \times 10^{-3}$ by unpaired t-test for AUC. Shaded box indicates PWV values (4-6 m/s) for HFHS-fed mice in comparable ranges of MAP (100-130mmHg), adapted from reference ²².

Figure 3. VSM *Bcl11b* deletion increases contractile force of aortic rings and arterial stiffness. (A) Representative force tracings recorded *ex vivo* in organ baths in aortic rings from WT (n=5) and BSMKO (n=7) mice. Scale on graph. Scatter plots indicate individual values for (B) force (mg), *, $p=6.0 \times 10^{-3}$; (C) wall tension (N/m), *, $p=2.0 \times 10^{-2}$; (D) stress (kPa), *, $p=3.0 \times 10^{-2}$; (E) stiffness, expressed as pulse wave velocity calculated via the Moens-Kortweg equation (PWV^{MK}), *, $p=4.0 \times 10^{-2}$; (F) KCl-, $p=7.5 \times 10^{-1}$, and (H) phenylephrine (PE)-induced stress (kPa), $p=2.9 \times 10^{-1}$. Each dot represents an aortic ring from one mouse; mean \pm SEM on graphs. (E) Pulse wave velocity (m/s) measured *in vivo* by Doppler echocardiography in WT (n=14) and BSMKO (n=17) mice. *, $p=4.0 \times 10^{-2}$ by unpaired t-test. Details in Methods.

Figure 4. cGMP-PKG-signaling pathway is down-regulated in aortas with VSM *Bcl11b* deletion. (A) Venn diagram of genes differentially up- and down-regulated in aortas of BSMKO (n=5) compared to WT (n=5) mice assessed by RNA sequencing. (B) Volcano plot of differentially up- (red) and down- (blue) regulated genes in aortas of BSMKO (n=5) compared to WT (n=5) mice. The horizontal line indicates a threshold of $p = 0.05$. For a list of the top 40 differentially regulated genes see Supplemental Figure IV. (C) List of genes within the cGMP-PKG-signaling pathway, the most significantly regulated

signaling pathway in BSMKO aortas after DAVID network analysis of differentially expressed genes (FDR $q=0.0094$). For quantitation of individual genes see Supplemental Figure VI. **(D)** Quantitative RT-PCR for guanylyl cyclase isoforms *Gucylal*, *Gucyla2* and *Gucylb1* in mRNA extracts from WT and BSMKO VSM cells. $n=4$ replicate experiments. Data expressed as fold change versus WT. *, $p=2.8 \times 10^{-2}$; †, $p=1.6 \times 10^{-2}$; ‡, $p=2.8 \times 10^{-2}$ by Mann-Whitney non-parametric test. **(E)** Representative Western Blot for PKG1 protein levels in VSM cells from WT and BSMKO mice. GAPDH used as loading control. Quantitation of 4 replicate experiments in graph. *, $p=3.0 \times 10^{-2}$ by Mann-Whitney non-parametric test. **(F)** Representative Western Blot for PKG1 in mouse VSM cells treated with a scrambled siRNA (control) or a validated *Bcl11b* siRNA. Quantitation of 3 replicate experiments on 3 different mouse VSM cell lines in graph. β -tubulin used as loading control. *, $p=4.0 \times 10^{-2}$ by unpaired t-test.

Figure 5. VSM *Bcl11b* deletion is associated with pVASP^{S239} downregulation in aortas. **(A)** VASP phosphorylation at serine 239 (pVASP^{S239}) was significantly decreased in BSMKO VSM cells, cultured with or without FBS, compared to WT cells. Total VASP remained unchanged. GAPDH serves as loading control. $n=5$ replicate experiments. *, $p=8.0 \times 10^{-3}$ by Mann-Whitney non-parametric test. **(B)** Representative Western Blot images demonstrating pVASP^{S239} in aortas of BSMKO mice ($n=6$) compared to WT littermate controls ($n=6$). β -actin serves as loading control. Each lane represents one mouse. *, $p=5.3 \times 10^{-5}$ by unpaired t-test. **(C)** pVASP^{S239} was significantly decreased in aortas of HFHS-fed mice ($n=10$) compared to ND-fed controls ($n=6$) (Same aortic samples as in Figure 2B). Total VASP was similar in the two groups. Each lane represents one mouse. Band intensity quantitation summarized in graphs. *, $p=9.6 \times 10^{-5}$ by unpaired t-test.

Figure 6. Calcineurin regulates VASP^{S239} phosphorylation after VSM *Bcl11b* deletion. **(A)** Representative Western Blot images demonstrating increased calcineurin (PP2B) expression, increased NFAT2 and impaired VASP phosphorylation at serine 239 (pVASP^{S239}) in BSMKO VSM cells compared to WT controls. GAPDH serves as loading control. Each lane represents a cell preparation from one mouse for a total of 4 replicates. **(B)** Treatment of BSMKO VSM cells with 1 or 10 μ M cyclosporine A (CsA), a calcineurin inhibitor, or **(C)** a specific calcineurin autoinhibitory peptide (CAIP, 10 or 100 μ M) reversed pVASP^{S239} in BSMKO cells towards WT levels, in a dose-dependent manner. V, vehicle control. Quantitation of band intensities in graph ($n=3$ replicate experiments). *, $p=1.5 \times 10^{-2}$ vs WT/vehicle; †, $p=3.0 \times 10^{-2}$ vs BSMKO/vehicle by one-way ANOVA with Tukey's multiple comparisons test. **(D)** Western Blots for *Bcl11b*, PKG1, PP2B and pVASP^{S239} in WT and BSMKO aortic media (adventitia removed) without (*left*) or with (*right*) transient transfection with vehicle (Lipofectamine; C, control) or 20 μ g *Bcl11b* plasmid. GAPDH serves as loading control.

Figure 7. VSM BCL11B regulates cytoskeletal actin polymerization and pVASP^{S239}. **(A)** Representative Western Blot images of F and G actin in WT ($n=6$) and BSMKO ($n=7$) aortas. F/G actin ratio quantitation in graph. *, $p=2.0 \times 10^{-2}$ by unpaired t-test. **(B)** Representative Western Blot images of α -actinin in WT ($n=4$) and BSMKO ($n=4$) aortas. Each lane represents one mouse. GAPDH used as loading control. Quantitation in graph. *, $p=3.0 \times 10^{-2}$ by Mann-Whitney non-parametric test. **(C)** Representative Western Blot images of F and G actin in BSMKO aortas treated with vehicle ($n=4$) or CAIP (10 μ M) ($n=4$). F/G actin ratio quantitation in graph. *, $p=5.0 \times 10^{-2}$ by Mann-Whitney non-parametric test. **(D)** Treatment of BSMKO aortas with CAIP (10 μ M) decreased stiffness, measured ex vivo on aortic rings in organ bath ($n=4$). *, $p=3.0 \times 10^{-2}$ by Mann-Whitney non-parametric test.

Figure 8. Cerebral microbleeds in WT vs BSMKO mice. **(A)** Representative magnetic resonance imaging (MRI) of whole brains from WT ($n=5$) and BSMKO mice ($n=6$). A microbleed-rich region is highlighted with the white box. Quantitation in graph. **, $p=1.0 \times 10^{-2}$ by unpaired t-test. **(B)** Representative histological staining of WT ($n=12$) and BSMKO ($n=12$) brain sections (40X magnification); areas stained in blue are indicative of cerebral microbleeds. Quantitation in graph (μm^2). Each dot represents the average of at least 5 sections, corresponding to a cumulative thickness of 150 μ m,



for each mouse. *, $p=3.0 \times 10^{-2}$ by unpaired t-test. (C) Representative histological staining of cerebral microbleeds in normal diet (ND)- (n=6) and high fat, high sucrose (HFHS)-fed (n=6) mice. Quantitation in graph. *, $p=5.0 \times 10^{-2}$ by unpaired t-test.



Circulation Research

NOVELTY and SIGNIFICANCE

What Is Known?

- Arterial stiffness is a strong, independent risk factor for cardiovascular disease (CVD); however genetic and molecular determinants of arterial stiffness are not fully understood, hampering the discovery of potential therapeutic targets to prevent CVD.
- Single nucleotide polymorphisms (SNPs) in a genetic locus on chromosome 14, upstream of the gene *BCL11B*, have been shown to be significantly associated with increased pulse wave velocity (PWV), the gold standard measure of aortic wall stiffness ($p < 5.6 \times 10^{-11}$ for the top SNP, rs1381289C>T).

What New Information Does This Article Contribute?

- We identified *BCL11B* in the vascular smooth muscle (VSM) as a novel and crucial regulator of vascular stiffness.
- VSM *BCL11B* contributes to maintaining aortic compliance via the cGMP/PKG/pVASP^{S239} signaling pathway, whose impairment, in absence of *Bcl11b*, leads to increased non-muscle actin polymerization in VSM cells and increased VSM stiffness.
- Increased aortic stiffness is associated with increased cerebral microbleeds, underscoring the pivotal role of large elastic arteries in preventing microvascular damage and associated target organ damage.

SNPs in a genetic locus on chromosome 14, known to function as an enhancer for the transcription factor *BCL11B*, are significantly associated with increased PWV, the gold standard measure of aortic wall stiffness. Here we report, for the first time, that *BCL11B*, previously known uniquely for its role in T-cell and neuronal lineage commitment, is present in VSM where it regulates vascular stiffness. Specifically, *BCL11B* modulates VSM cytoskeletal actin polymerization via the cGMP/PKG/pVASP^{S239} signaling pathway thereby regulating aortic stiffness. Notably, increased arterial stiffness in mice lacking VSM *Bcl11b* as well as in obese mice, a mouse model of arterial stiffness we previously described, is associated with increased incidence of cerebral microbleeds, suggesting a crucial role of large elastic arteries in preventing microvascular damage in downstream organs. Interestingly, despite profound effects on the aorta, *BCL11B* has a dispensable role in VSM contraction in resistance arteries. The present study strongly supports *BCL11B* or its downstream regulated pathways as potential therapeutic targets against arterial stiffness and related target organ damage, to prevent overt CVD, which remains a major cause of morbidity and mortality worldwide.

Figure 2

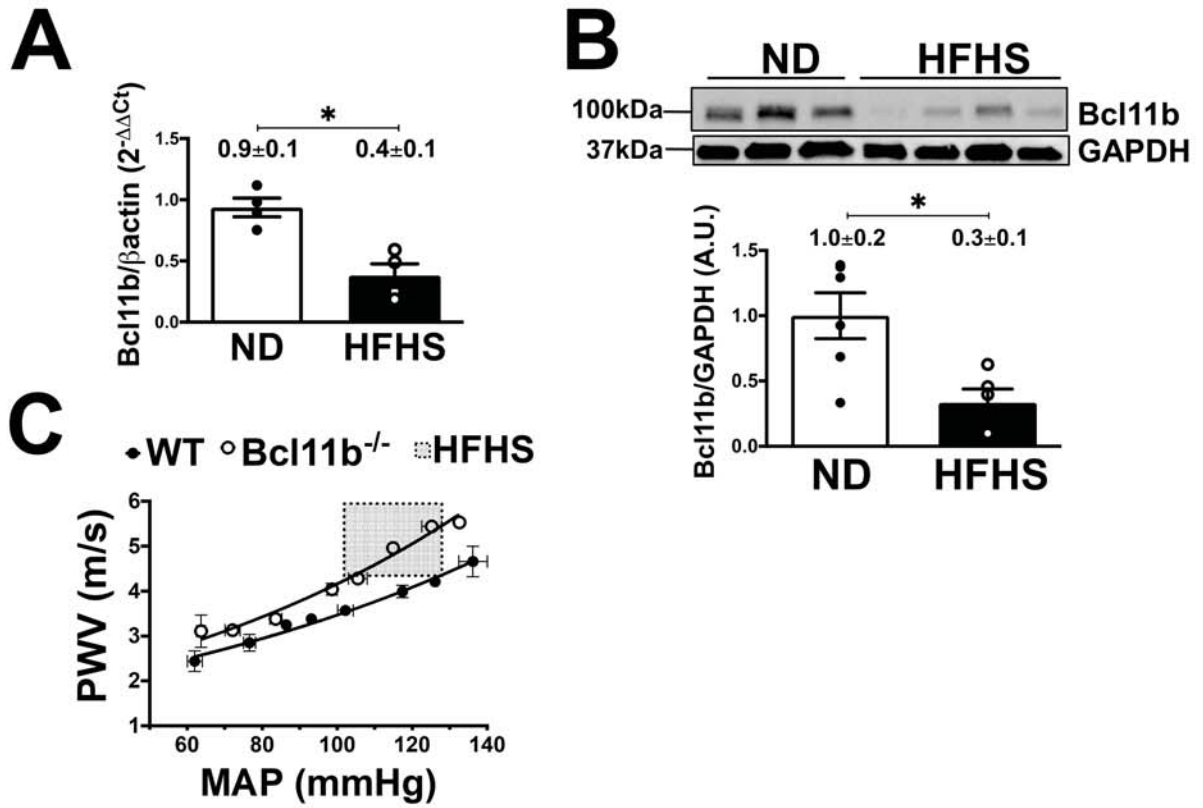


Figure 3

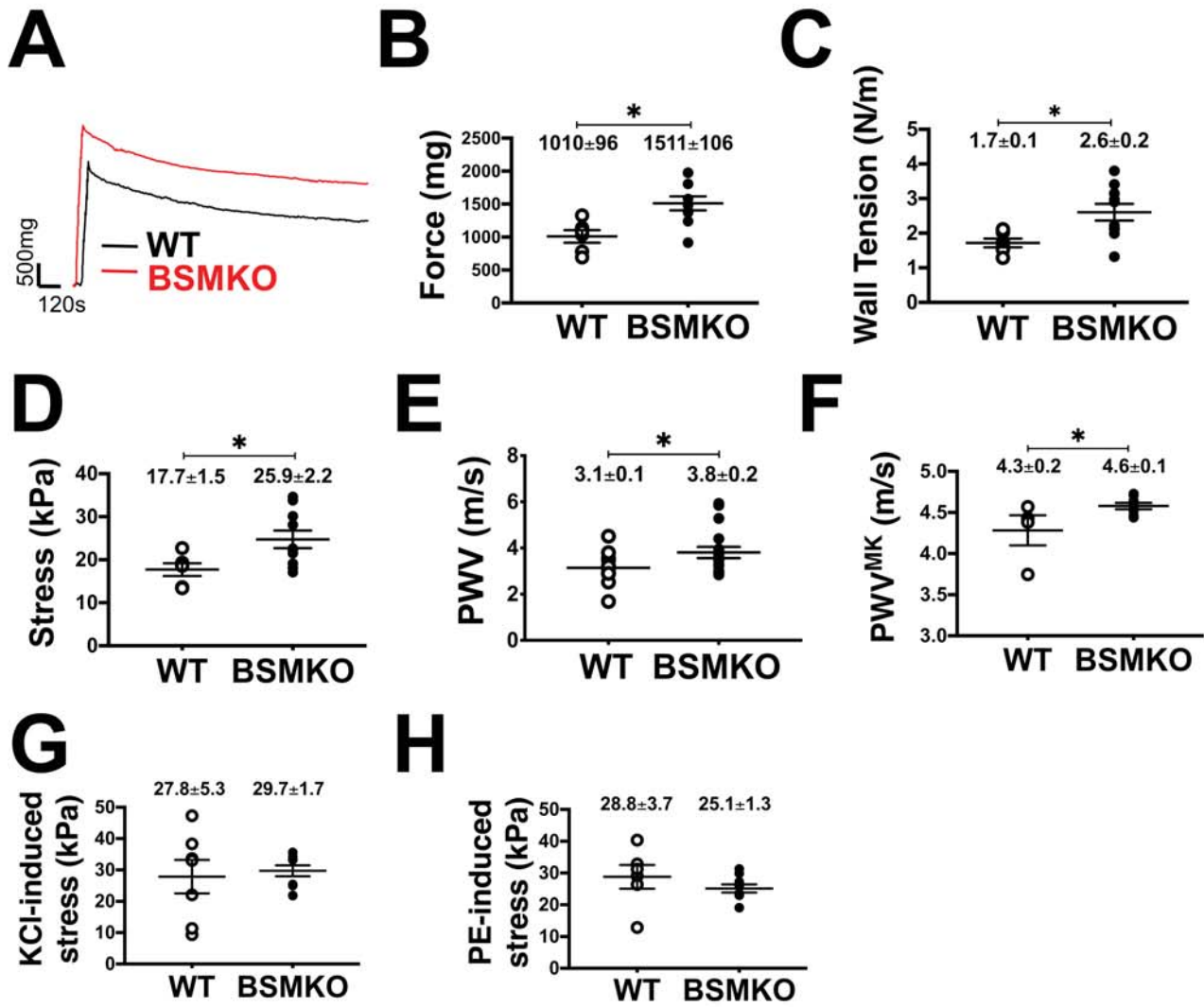


Figure 4

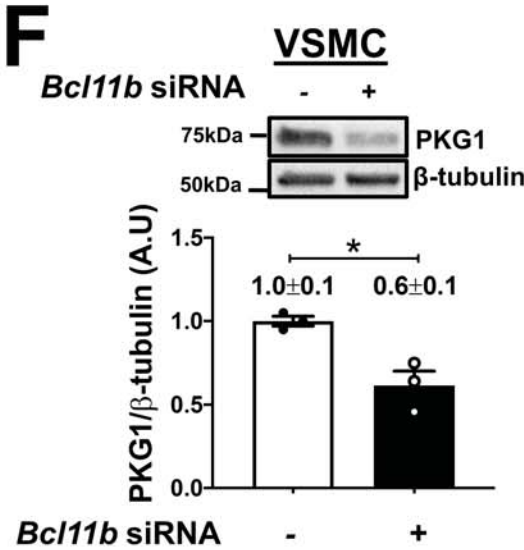
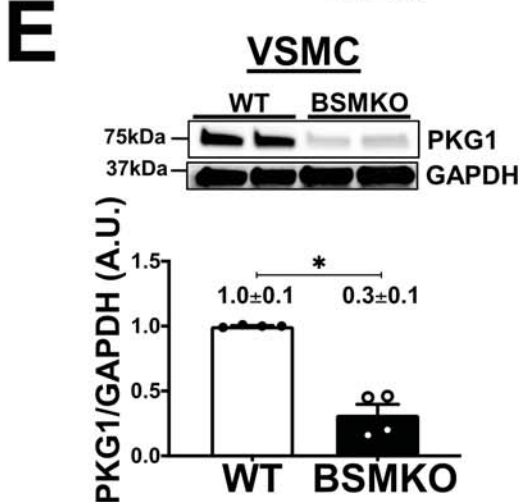
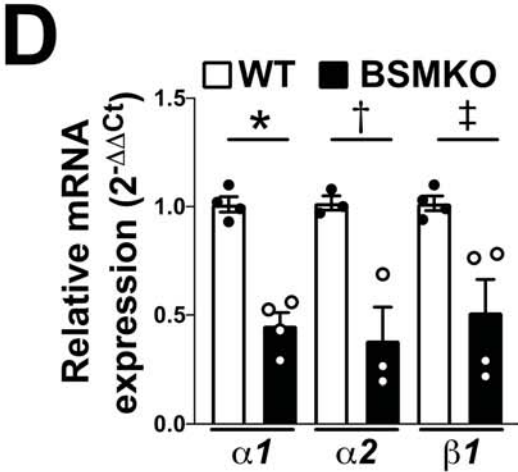
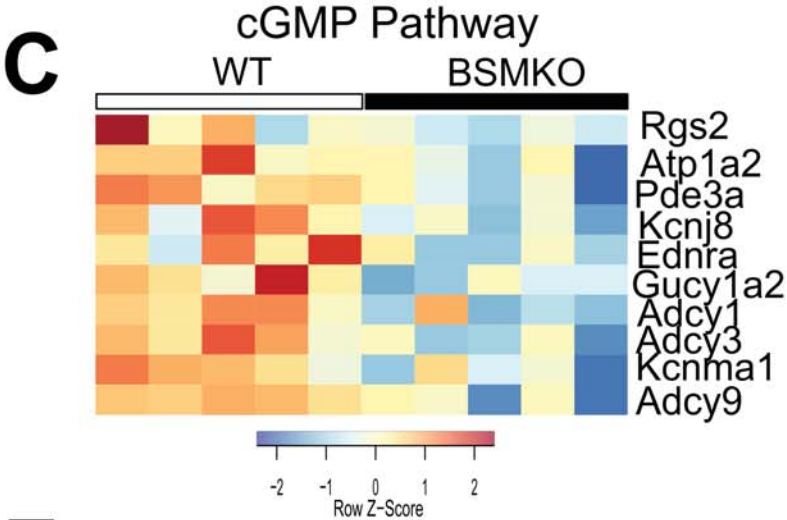
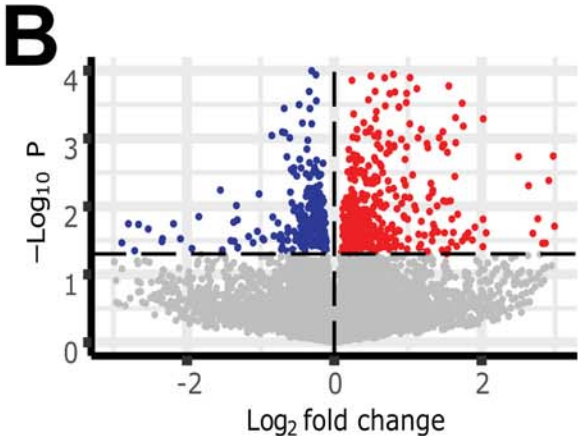
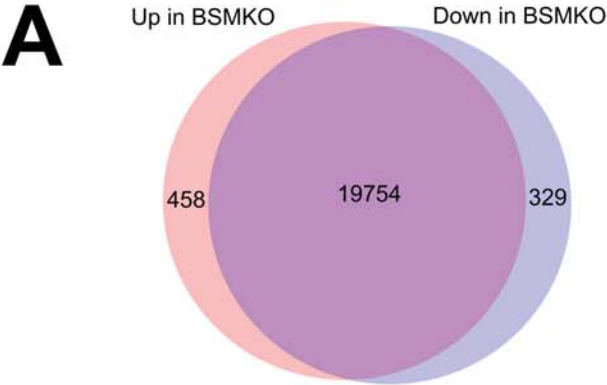
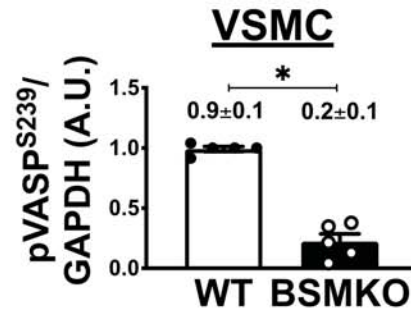
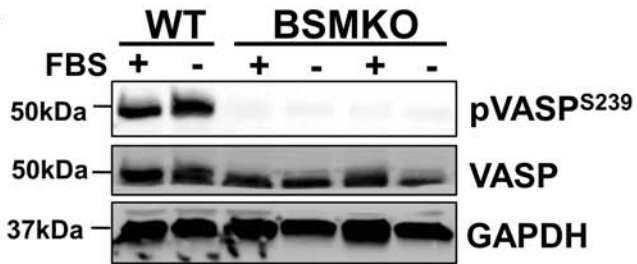
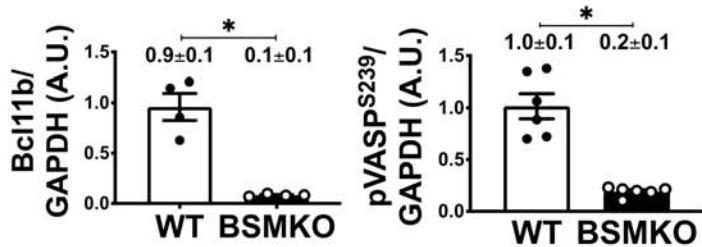
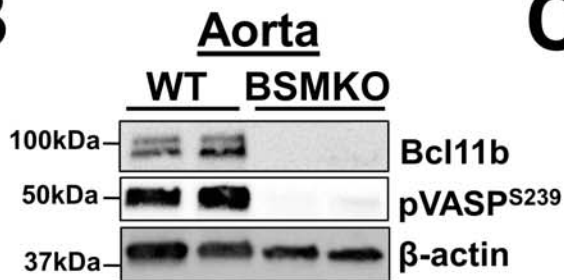


Figure 5

A



B



C

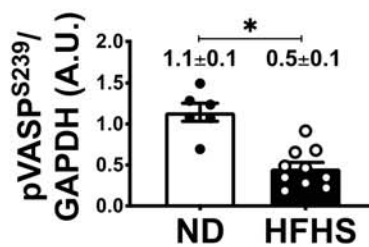
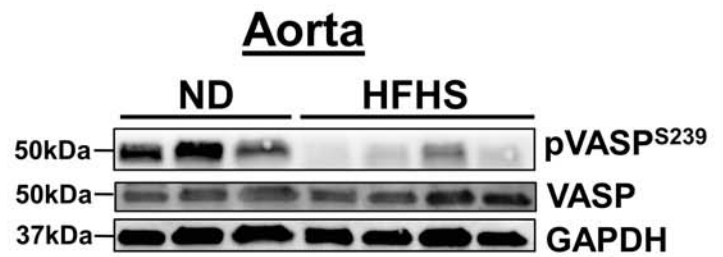


Figure 6

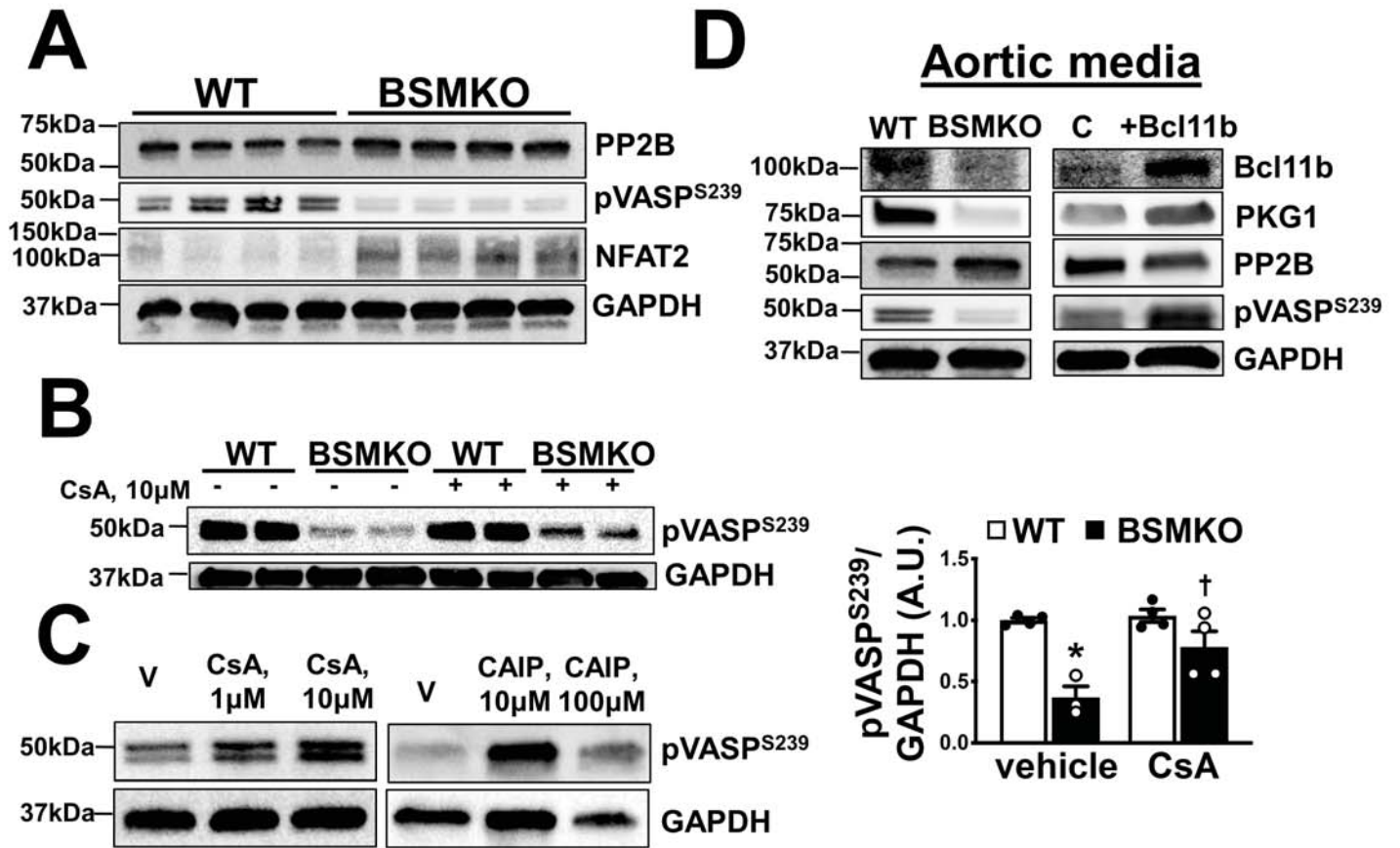


Figure 7

